A simulation of QCD radiation in top quark decays

Keith Hamilton and Peter Richardson

Institute of Particle Physics Phenomenology, Department of Physics
University of Durham, Durham, DH1 3LE, U.K.
E-mail: `keith.hamilton@durham.ac.uk`, `peter.richardson@durham.ac.uk`

ABSTRACT: In this paper we describe a theoretical framework and algorithms for implementing QCD corrections to top quark decays in the Herwig++ event generator. The dominant corrections, due to soft and collinear emissions, are summed to all orders through the coherent parton branching formalism. In addition, unenhanced first-order matrix-element corrections are included to account for large transverse momentum emissions.

Contents

1. Introduction

In the coming era particle physics experiments will probe ever greater energies so naturally top quark physics will play an increasingly important rôle in experimental and theoretical studies. A major area of study at forthcoming collider experiments will be the precision measurement of the top quark mass, which is one of the fundamental input parameters of the standard model and gives rise to the leading contributions to its effective potential. In addition, a thorough understanding of top quark physics is crucial for the discovery of new heavy particles, most notably the Higgs boson, since, due their copious rate of production, top quarks will provide the main source of standard model background.

Although inclusive quantities such as total cross sections are well described by fixed-order QCD calculations, experimental analyses require a detailed description of the final state. Large logarithmic contributions to differential distributions must be resummed to all orders and hadronization effects taken into account. Parton shower Monte Carlo simulations include these higher-order corrections by appealing to the strongly ordered soft/collinear limit in which higher-order matrix elements are represented by universal factors multiplying the lowest order matrix element. This leading-log approximation scheme may be recast in a probabilistic form, a Markov chain, from which we can attempt to generate events as they occur in nature.

In this paper we will describe such a prescription for the simulation top quark decays, implemented in the new Herwig++ event generator [1, 2]. Many issues raised here and aspects of the physics we present are also relevant to a discussion of radiation from the top quark in its production. In full generality it is not possible to study the production and decay phases separately, doing so corresponds to working in the *narrow width approximation*, i.e. neglecting the width of the top quark. In practice this means the width of the top quark, which is of order $1\,\mathrm{GeV}$, should be considered infinitesimal and so we should not simulate gluons with energies below that scale. This does not present a problem as such a scale is already approximately equal to the typical cut-off scale used to terminate the parton shower (the scale at which the parton shower hands over to the hadronization model).

Simulations of this process have been considered in the past, in the older FORTRAN HERWIG program [3, 4]. The simulation which we describe improves on this earlier work in a number of ways, partially due to general theoretical developments [5, 6]. The older HERWIG program was based on a non-covariant showering formalism. This meant that, working in the top quark rest frame, the top quark could emit no radiation before it decayed. Consequently the entire phase-space had to be populated as though all emissions originated from the b-quark. In addition, the older program had grown out of a formalism based on massless emitting partons which forced the introduction of an *ad hoc* angular cut-off on gluon emission, giving rise to an unphysical *halo* of gluons at small angles [7].

In this paper we describe an approach based on a new covariant parton showering formalism, which naturally includes gluon radiation from the decaying top quark [5]. This has the advantage that the region of phase space corresponding to soft gluon emission is populated exclusively by the parton shower, instead of the single gluon emission matrix element, as in earlier simulations, which required an *ad hoc* soft cut-off [3, 4]. Another significant benefit of this new formalism is that it enables a correct treatment of the masses of the emitting partons through the use of quasi-collinear splitting functions: no angular cut-off is required.

Finally we note that the standard coherent parton shower algorithm has two important drawbacks. Firstly, because the parton shower generates emissions from each leg of the hard scattering (quasi-) *independently*, each additional emission must be *uniquely* associated to a particular leg of the hard scattering, which can only be achieved at the price of having regions of phase space, corresponding to high p_T gluon emissions, which are unpopulated by the shower. Secondly, the soft/collinear approximation to the QCD matrix elements is
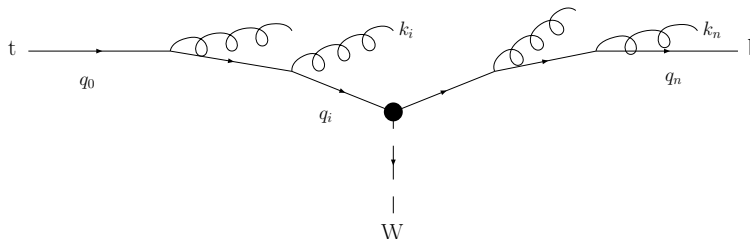
Figure 1: An example of the decay $t \to bW + (n)\, g$.

not a good approximation all over the phase-space region populated by the parton shower. Both of these problems may be solved by so-called *matrix element corrections* [8] which ensure that the hardest additional gluon emission in the event is distributed according to the *exact* matrix element. We discuss the inclusion of these corrections in the approach of [5] which leads to significant improvements in predictions of physical observables.

In the next section we present the basic parton shower formalism, based on the covariant parton shower formalism described in [5]. As we are using the parton shower approximation in a range of kinematics and masses that it has not been used in before[1] our discussion is accordingly detailed. The inclusion of the matrix element correction to the decays is considered in section 3 followed by a discussion of the results of the simulation in section 4. Finally we present our conclusions and plans for further developments.

2. Basic shower formulation for $t \to bW$ decays

Unlike other quarks, the mass and width of the top quark are such that it emits radiation and decays before hadronization occurs [9, 10]. In this section we describe the parton shower approximation to the decay of a top quark to a W boson and a b-quark with additional gluon radiation. Here we are only concerned with the *decay* of the top quark, that is our initial state is an *on-shell* top quark produced in some hard scattering process.

2.1 Shower variables

We use the conventions and shower variables described in [5], which we briefly review here; these variables, together with an appropriate ordering condition for multiple emissions, ensure that the emissions obey the angular ordering of QCD radiation.

The decay $t \to bW + (n)\, g$ is depicted in figure 1. The parton showers may be viewed as cascades of quarks decaying to quark-gluon pairs: $q_{i-1} \to q_i + k_i$. The momenta of the quarks and gluons in the shower are defined in terms of the following Sudakov decomposition

$$
\begin{aligned}
q_i &= \alpha_i p + \beta_i n + q_{\perp i}, \\
k_i &= q_{i-1} - q_i.
\end{aligned}
\tag{2.1}
$$

As usual in parton shower simulations, prior to simulating gluon emissions the leading order decay must be generated. The initial (on-shell) top and bottom quark momenta

---

[1]In the earlier work of [3] only the b-quark radiated.

serve to define the basis vectors p needed for each shower. The n and $q_{\perp i}$ basis vectors are defined in the rest frame of the initial top quark with the initial b-quark momentum in the z direction. In this frame the n vectors for top and b-quark showers are chosen to be

$$
\begin{aligned}
n_t &= \tfrac{1}{2}m_t\left(1,\mathbf{0},1\right), \\
n_b &= \tfrac{1}{2}m_t\left(\lambda,\mathbf{0},-\lambda\right),
\end{aligned}
\tag{2.2}
$$

where λ is given by,

$$
\lambda = \frac{1}{m_t^2}\sqrt{m_t^4 + m_W^4 + m_b^4 - 2m_t^2 m_b^2 - 2m_t^2 m_W^2 - 2m_W^2 m_b^2}.
\tag{2.3}
$$

The $q_{\perp i}$ vectors have the form $(0,\mathbf{q}_{\perp i},0)$ in this frame.

In addition to the Sudakov decomposition (2.1) we also adopt the following variables from [5] for the top quark shower

$$
\begin{aligned}
\tilde{q}_i^2 &= \frac{m_t^2 - q_i^2}{1-z_i}, & z_i &= \frac{\alpha_i}{\alpha_{i-1}}, \\
p_{\perp i} &= q_{\perp i} - z_i q_{\perp i-1}, & \mathbf{p}_{\perp i}^2 &= -p_{\perp i}^2,
\end{aligned}
\tag{2.4}
$$

where $p_{\perp i}$ is defined to be the relative transverse momentum involved in branching i, and $\tilde{q}_i^2$ is the *evolution variable*. For radiation from the bottom quark the definitions in (2.4) are unchanged except for the evolution variable, which becomes

$$
\tilde{q}_i^2 = \frac{q_{i-1}^2 - m_b^2}{z_i\left(1-z_i\right)}.
\tag{2.5}
$$

These evolution variables $\tilde{q}_i^2$ are defined by close analogy to those of the original HERWIG program [4], they correspond closely to the angle between the emitted quark and gluon: ordering in $\tilde{q}_i^2$ results in angular ordering of both the top quark and bottom quark parton showers. This feature is discussed in more detail in section (2.3).

2.2 Shower phase space

We begin by considering the decay $t \to bW + (n)\,g$, where the gluons are *unresolved*. The partial width for such a decay is given by

$$
\int \mathrm{d}\Gamma_n = \frac{1}{2m_t}\int \mathrm{d}\Phi_{bW}\mathrm{d}\Phi_K\ (2\pi)^4\,\delta^4\left(p_t - q_b - q_W - K\right)\left|\mathcal{M}_n\right|^2,
\tag{2.6}
$$

where m_t is the mass of the top, p_t is its four-momentum and $q_{b/W}$ is the four-momentum of the b/W. We have also denoted the matrix element $\mathcal{M}_n$. K denotes the sum of the individual gluon momenta $\sum_{i=1}^n k_i$, while $\mathrm{d}\Phi_K$ and $\mathrm{d}\Phi_{bW}$ are the phase-space measures for the gluon and bW systems respectively,

$$
\begin{aligned}
\int \mathrm{d}\Phi_K &= \prod_{i=1}^n \int \mathrm{d}\Phi_{k_i} = \prod_{i=1}^n \int_{\mathcal{U}} \frac{\mathrm{d}^3 k_i}{(2\pi)^3 2k_i^0}, \\
\int \mathrm{d}\Phi_{bW} &= \prod_{i=b,W} \int \frac{\mathrm{d}^3 q_i}{(2\pi)^3 2q_i^0}.
\end{aligned}
\tag{2.7}
$$

The symbol $\mathcal{U}$ denotes the region of phase space *inside* which gluons are unresolvable.

Assuming the branching picture depicted in figure 1, the full phase space may be factorised by repeatedly inserting the identity as integrals over two simple delta functions, one such insertion for each gluon vertex:

$$\int d\Phi_{bW} d\Phi_K = \prod_{i=1}^n \int d\Phi_i \int d\Phi_{bW} (2\pi)^4 \delta^4 (q_i - q_{i+1} - q_W)$$
$$\int d\Phi_i = \int d\Phi_{k_i} d^4 q_i dQ_i^2 \delta \left(Q_i^2 - q_i^2 \right) \delta^4 (q_{i-1} - q_i - k_i)$$
$$\tag{2.8}$$

where $q_0 = p_t$, $q_n = q_b$. Given the branching picture in figure 1, the parton showers may be viewed as cascades of two body decays $q \to qg$. This interpretation is evident from the fact that $d\Phi_i$ has the familiar form of a two body phase-space measure for a quark of mass Q_i and a gluon, albeit with an additional Q_i^2 integration.

Exploiting the Lorentz invariance of the integration measure, we may rewrite the two body phase-space integrals for the top quark (2.8) as

$$\int d\Phi_i = \frac{1}{4 (2\pi)^2} \int d\tilde{q}_i^2 dz_i \ (1 - z_i), \tag{2.9}$$

these differ from those of the b-quark by a factor of z_i due to slightly different definitions of the evolution variables (2.4), (2.5).

2.3 Soft gluon coherence and angular ordering

The integration limits on $\tilde{q}_i^2$ and z_i in (2.9) may be inferred from the kinematic constraints involved in each splitting, however, as we shall now discuss, *dynamical*, soft gluon interference, effects motivate further restrictions on this phase space and hence a modification to the integration bounds implied by the kinematics.

Using the soft gluon insertion technique [11], and following a similar analysis to that in [12], the squared amplitude for a soft gluon dressing the decay $t \to bWg$, with amplitude $\mathcal{M}_1$, is given by

$$\lim_{k \to 0} |\mathcal{M}_2|^2 = \frac{2g_s^2}{\omega^2} \begin{pmatrix} C_F \left(W_{tg}^t + \tilde{W}_{gb}^t - \tilde{W}_{tb}^g + \tilde{W}_{gt}^b \right) \\ + C_F \left(\tilde{W}_{gb}^t + \tilde{W}_{tb}^g + \frac{1}{2} W_{tb}^b + \frac{1}{2} W_{bg}^b \right) \\ + C_A \left(W_{tg}^g + \tilde{W}_{tb}^g - \tilde{W}_{gb}^t + \tilde{W}_{tg}^b \right) \end{pmatrix} |\mathcal{M}_1|^2 \tag{2.10}$$

where

$$W_{ij}^i = \frac{1}{2n_i.n_k} \left(1 - \frac{n_i^2}{n_i.n_k} + \frac{n_i.n_j - n_i.n_k}{n_j.n_k} \right),$$
$$\tilde{W}_{jk}^i = \frac{1}{2} \left(W_{ik}^i - W_{ij}^i \right), \tag{2.11}$$

ω is the energy of the soft gluon, $n_i = p_i/E_i$, $n_k = k/\omega$, and the sum over colours and spins, is understood. The first two terms proportional to C_F are due to (incoherent) radiation from the top quark and bottom quark respectively, the third term, proportional to C_A, is due to radiation from the hard gluon (g). Averaging W_{ij}^i over the azimuthal angle, about p_i, one readily finds

$$\langle W_{ij}^i \rangle = \frac{1}{2n_i.n_k} \left(1 - \frac{n_i^2}{n_i.n_k} + \frac{v_i (n_i.n_j - n_i.n_k)}{\sqrt{(n_i.n_j - n_i.n_k)^2 - n_j^2 \left((1 - n_i.n_k)^2 - v_i^2 \right)}} \right), \tag{2.12}$$

where $n_i^2 = 1 - v_i^2$, with v_i the velocity of particle i. Clearly in the limit $v_i, v_j \to 1$, we see that the emission from i in a pair of partons ij is restricted to a cone *viz*

$$\langle W_{ij}^i \rangle = \frac{1}{2n_i.n_k} \theta \left(\theta_{ij} - \theta_i \right), \tag{2.13}$$

where θ_i is the angle between the soft gluon and i, and θ_{ij} is the angle between i and j. The vanishing of the radiation outside the cone is attributable to destructive interference.

To demonstrate the angular ordering of the radiation from the top quark we need to consider the limit in which the directions of the top quark and hard gluon approach one another. We also need to consider $v_t, v_b \to 1$ in order to use (2.13). In the dipole rest frame (the rest frame of the W boson) v_t is around 0.7, so the validity of working in the limit $v_t, v_b \to 1$ is questionable, we will address this matter shortly. Proceeding with these approximations we find $n_g = n_t$ and hence

$$\begin{aligned}
|\mathcal{M}_2|^2 &= \frac{2g_s^2}{\omega^2} \left(C_F W_{tg}^t + C_A W_{tg}^g + C_F W_{t^*b}^b + C_F \tilde{W}_{t^*b}^{t^*} \right) |\mathcal{M}_1|^2 \\
W_{t^*b}^b &= \frac{1}{2} \left(W_{tb}^b + W_{bg}^b \right) \\
\tilde{W}_{t^*b}^{t^*} &= \frac{1}{2} \left(W_{tb}^t - W_{tg}^t \right) + \frac{1}{2} \left(W_{gb}^g - W_{gt}^g \right)
\end{aligned} \tag{2.14}$$

The first two terms in the radiation pattern (2.14) are due to (incoherent) emissions from the top quark and hard gluon respectively. The third term in the radiation pattern is due to (incoherent) radiation from the b-quark, due to its interaction with t^*, by which we mean the amalgamation of t and g (soft gluon emissions from b will not 'resolve' the separation of t and g). In the limit $v_t, v_b \to 1$, the azimuthal average of each of the first three terms, of the form W_{ij}^i, is given by (2.13), so soft gluon emissions are restricted to cones whose half angle is equal to that between the two particles forming the colour dipole (i and j).

Similarly, by virtue of (2.13), the radiation due to the fourth term in (2.14) is restricted to a *wide* cone lying along the t^* direction, reaching out to the b-quark, but with emissions *vetoed* in the smaller cones, where the incoherent t and g emissions are allowed. The radiation due to the fourth term is considered to be the coherent sum of emissions from t and g (2.14) and therefore, equivalently, soft, angular ordered, wide angle, radiation from the internal, off-shell t^* line. This analysis indicates that in evolving toward the decay, from the on-shell top quark, the angle of the emissions is always increasing.

We now turn to question the validity of using the $v_t, v_b \to 1$ limit in motivating this angular ordering. In [7] it was found that *equal* finite parton masses in $\langle W_{ij}^i \rangle$ smooth the angular cut-off provided by the step function in (2.13) to the form shown in brackets in (2.12), also the finite masses screen the collinear singularity in the $2n_i.n_k^{-1}$ prefactor giving rise to the so-called *dead-cone* effect [7].

In the case of the $t \to bW$ decay, assigning velocities to t and b like those in the W rest frame, the dead-cone effect is pronounced but the smoothing of the $\theta \left(\theta_{tb} - \theta_t \right)$ cut-off does not occur, as one can see from the plot of $\langle W_{tb}^t \rangle$ in figure 2. On the other hand, in the $t \to bW$ case, the radiation distribution does not simply vanish outside the cone like $\theta \left(\theta_{tb} - \theta_t \right)$ but rather it can be negative for small θ_{tb}. Therefore, by performing
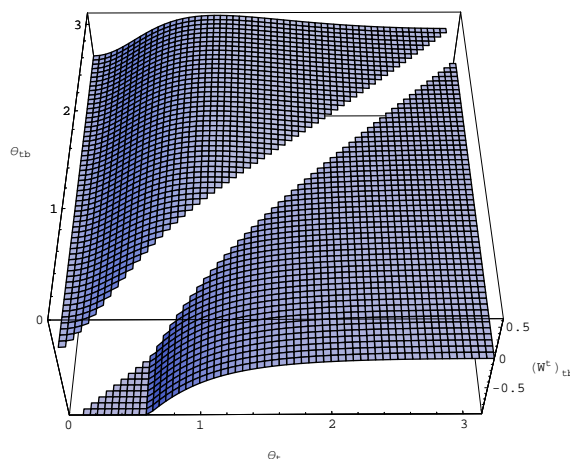
Figure 2: In this figure we show the azimuthally averaged radiation pattern $\langle W_{tb}^t \rangle$, for $v_t = 0.65$, $v_b = 1$. In this plot, the ratio of the integral of $\langle W_{tb}^t \rangle$ outside the cone, to the same integral inside the cone is around -0.33.

conventional angular ordering, we will be making an approximation i.e. neglecting this negative contribution. We argue, as in [7], that this is justified given that the majority of the radiation is inside the cone: for $v_t \approx 0.7$, $v_b \approx 1$, as in figure 2, we find that the ratio of the integral of $\langle W_{tb}^t \rangle$ outside the cone to the same integral inside the cone is approximately -0.3.

The same calculation can be performed for the b-quark in the limit $v_b \to 1$ and one finds that the emission angles are required to be successively smaller as one evolves away from the decay.

In terms of the $\tilde{q}_i$ evolution variable, in the top quark rest frame, in the soft limit $(1 - z = \epsilon)$, one may show that

$$\frac{\tilde{q}_t^2}{m_t^2} = \frac{2}{1 - \cos \theta_b}, \tag{2.15}$$

where θ_b is the angle between the soft gluon and the b-quark (since the top is at rest) i.e. starting at $\tilde{q}_0^2 = m_t^2$ and evolving to higher values monotonically increases the angle/transverse momentum of the soft gluon emission with respect to the b-quark direction. This is consistent with our analysis of the soft radiation pattern from the $t \to bWg$ decay (2.14), in the W boson rest frame, which is obtained by a boost in the W boson direction, which will preserve the transverse momentum ordering. Therefore implementing angular ordering in the top quark shower simply involves bounding $\tilde{q}_{i+1} > \tilde{q}_i$. For the b-quark the situation is the same as in the older HERWIG program namely $\tilde{q}_{i+1} < z_i \tilde{q}_i$. These bounds give rise to nested $\tilde{q}_i^2$ phase-space integrals. Finally we note that this ordering in $\tilde{q}_i^2$ is more stringent than the q_i^2 ordering implied by the kinematics, one may easily prove that the q_i^2 ordering is a byproduct of the $\tilde{q}_i$/angular ordering using just the definitions in section (2.1).

2.4 Matrix element approximations

Thus far we have shown how the phase space for the parton shower may be exactly factorized in a Lorentz invariant way. We will now briefly discuss the factorization of the n-parton matrix element.

The principle requirement for factorization of the matrix element is that the emissions are either soft or quasi-collinear or both. Such emissions are significantly favoured by the underlying dynamics and so the majority are of this type. We aim to accurately describe all quasi-collinear emissions and to take into account soft gluon emissions through the approximation of angular ordering.

2.4.1 Emissions from top quarks

The quasi-collinear limit [13] is defined to be the limit in which $\mathbf{p}_{\perp i}^2$ and the on-shell quark mass squared $\left(m_q^2\right)$ are assumed small compared to $n.p$ but not compared to each other. For an n-parton process in which a decaying top quark emits a quasi-collinear gluon, the squared matrix element factorizes according to

$$\lim_{q_n \parallel k_n} |\mathcal{M}_n|^2 = \frac{8\pi\alpha_{\mathrm{S}}}{(1-z_n)\,\tilde{q}_n^2} P_{qq}\left(z_n, \tilde{q}_n^2\right) |\mathcal{M}_{n-1}|^2, \tag{2.16}$$

$$P_{qq}\left(z, \tilde{q}^2\right) = C_F\left(\frac{1+z^2}{1-z} - \frac{2zm_t^2}{(1-z)\,\tilde{q}^2}\right), \tag{2.17}$$

where $\mathcal{M}_{n-1}$ is the matrix element for the process without the additional gluon emission. P_{qq} is the quasi-collinear quark-gluon splitting function [13].

Another important requirement for our factorization of the matrix element is that the gluon emissions are such that the intermediate quark virtualities are strongly ordered. As mentioned previously, the virtualities are naturally ordered by kinematics alone. Furthermore, from the Sudakov decomposition (2.1) and our definitions (2.2), one can show that imposing angular ordering automatically provides an ordering of virtualities which is more restrictive than that dictated by the branching picture in figure 1. For strongly ordered emissions the decomposition (2.16) may be applied recursively, reducing $|\mathcal{M}_n|^2$ to a product of splitting functions that multiply the leading-order matrix element.

Unfortunately, for emissions from the top quark, given our choice of n (2.2), $n.p = \frac{1}{2}m_t^2$. Therefore one may not expect that the quasi-collinear splitting function approximates the single emission matrix element very well. Although the choice of n is arbitrary, in the top quark rest frame $n.p$ only depends on the energy components of n and, as we shall see shortly (2.18), the quasi-collinear splitting function is invariant under rescalings of n. This is may be viewed as a manifestation of the fact that collinear enhancements usually take the form of large *mass singular* logarithms of some scale, characteristic of the leading order process, divided by the quark mass, whereas in this case the characteristic scale *is* the quark mass. This is, nevertheless, not a problem; the fact that the collinear emissions are suppressed means that only soft emissions are enhanced and, as we shall now demonstrate, these are well modelled by our approximations.

From the definition of the quasi-collinear splitting function and the shower variables z and $\tilde{q}^2$, we find that the approximation to the quasi-collinear limit of $|\mathcal{M}_n|^2$ can be

rewritten

$$\lim_{q_i \| k_i} |\mathcal{M}_n|^2 = 8\pi\alpha_{\mathrm{S}}C_F\mathcal{D}_{t,n}|\mathcal{M}_{n-1}|^2, \tag{2.18}$$

$$\mathcal{D}_{t,n} = \frac{1}{2q_{i-1}.k_i}\left(\frac{n.k_i}{n.q_{i-1}} + \frac{2n.q_i}{n.k_i} - \frac{n.q_i m_t^2}{(n.q_{i-1})(q_{i-1}.k_i)}\right). \tag{2.19}$$

In the soft limit the first term in $\mathcal{D}_{t,n}$ is sub-leading and may be neglected (k_i is only in the numerator), also in the soft limit $q_i = q_{i-1}$, so our approximation to $|\mathcal{M}_n|^2$ in the soft limit is

$$\mathcal{D}_{t,n} = \frac{n.q_t}{(q_t.k_i)(n.k_i)} - \frac{m_t^2}{2(q_t.k_i)^2}. \tag{2.20}$$

Neglecting the b-quark mass $n \equiv q_b$ and we may recognise this soft limit $\mathcal{D}_{t,n}$ as having *precisely* the familiar form of the eikonal dipole radiation function, namely,

$$\mathcal{D}_{t,n} = -\frac{1}{2}\left(\frac{q_b}{q_b.k_i} - \frac{q_t}{q_t.k_i}\right)^2. \tag{2.21}$$

Plainly, the quasi-collinear splitting function, together with the definition of n and the shower variables $(z, \tilde{q}^2)$, reproduces exactly the correct soft limit of $|\mathcal{M}_n|^2$ if one neglects the mass of the b-quark.

Taking into account the b-quark mass, the differences between the soft approximation we use (2.18) and the exact result (2.21) will become significant if there are emissions for which $q_b.k_i$ becomes small i.e. for emissions near-collinear to the b-quark. However such emissions are generated assuming that they were emitted by the b-quark, i.e. they are produced by the b-quark shower and not the top quark shower.

The high level of agreement between our approximation (2.18) and the exact soft distribution (2.21) is understandable given the size of the ratio m_b/m_t. Despite this nice feature, the distribution of radiation which is produced is nevertheless based on an approximation, in particular the distribution of high transverse momentum emissions is known to be modelled poorly. This matter will be rectified later through the soft-matrix element correction, to be discussed in section 3.

Finally, although, strictly speaking, a higher order effect, earlier studies, neglecting quark mass effects, have shown that a careful choice of scale for α_{S} enables one to include parts of the next-to-leading-log contributions [14]. More specifically, for light quarks, the soft $z \to 1$ limit of the P_{qq} massless splitting function at the two-loop order may be obtained by expanding $\alpha_{\mathrm{S}}\left(\mathbf{p}_{\perp i}^2 = (1-z)^2\,\tilde{q}^2\right)$ about q^2 to $\mathcal{O}\left(\alpha_{\mathrm{S}}^2\right)$ and rescaling $\Lambda_{\overline{\mathrm{MS}}}$. For massive partons we assume that the appropriate argument for α_{S} is again $(1-z)^2\,\tilde{q}^2$, which is equal to $\mathbf{p}_{\perp i}^2 + (1-z_i)^2\,m_t^2$. Although the argument of α_{S} is no longer the local transverse momentum and although the quasi-collinear splitting function contains a term not present in the massless case, in the limit $z \to 1$ both the argument of α_{S} and the quasi-collinear splitting function tend to their respective values in the massless analysis and so we can once again expect to reproduce the higher order terms.

2.4.2 Emissions from b-quarks

Gluon emissions from b-quarks are distributed according to the associated quasi-collinear splitting function, this is the same as (2.17) but for the replacements $z_i m_t^2 \to m_b^2$ and $\tilde{q}_i^2 \to z\tilde{q}_i^2$. As in the case of emissions from the top quark, we may express this factorization in terms of scalar products by using the Sudakov decomposition:

$$\lim_{q_i \| k_i} |\mathcal{M}_n|^2 = 8\pi\alpha_S C_F \mathcal{D}_{b,n} |\mathcal{M}_{n-1}|^2, \tag{2.22}$$

$$\mathcal{D}_{b,n} = \frac{1}{2q_i.k_i}\left(\frac{n.k_i}{n.q_{i-1}} + \frac{2n.q_i}{n.k_i} - \frac{m_q^2}{q_i.k_i}\right). \tag{2.23}$$

This splitting function accurately reproduces the distribution of gluons emitted at small angles to the quark, however, sizeable errors may occur if the approximation is used beyond the quasi-collinear limit.

Evidently emissions close to the n direction are enhanced by the second term in (2.23), proportional to $n.k_i^{-1}$. This enhancement is unphysical; as well as being a basis vector of the Sudakov decomposition, n is also the (axial) gauge vector used in the calculation of the quasi-collinear splitting functions. The manifestation of such divergences indicates a breakdown of the quasi-collinear approximation, i.e. emissions for which $q_{i-1}.k \ggg n.k_i$ are beyond the quasi-collinear limit.

As was shown for the case of the top quark shower, choosing n collinear with the colour partner gives a good approximation to the eikonal limit and assigns a physical origin to the $n.k^{-1}$ divergence. Unfortunately, for the case in hand we cannot choose n collinear with the top quark since we are in its rest frame and n is light-like. Instead we choose n acolinear with q_b, thereby maximally separating it from the region of phase space into which the shower can emit gluons. In spite of this, results show a substantial excess of high transverse momentum emissions from the b-quark, due to the $n.k_i^{-1}$ enhancement. This is later rectified by the soft matrix element correction procedure described in section 3.1.

Although the soft matrix element correction will compensate any excess emission, we would prefer that this was not the default *modus operandi*, since we only implement these process-specific corrections for cases of special interest. By generalizing the quasi-collinear splitting function to

$$P_{qq} \to \mathcal{V}_{qq} = P_{qq} - C_F\left(\frac{q_i.k_i}{n.k_i}\right)\frac{n^2}{n.k_i} \tag{2.24}$$

and setting $n = q_t$, we can also remedy the surplus emissions and generally improve the shower approximation. This modification produces the correct soft and collinear limits, it is similar in nature to a soft matrix element correction procedure [8]. Unlike the soft matrix element correction, the generalized quasi-collinear splitting function $\mathcal{V}_{qq}$ is process independent. In the most basic sense, our splitting function may be viewed as a simple merging of the quasi-collinear limit with the *full* eikonal limit of the colour dipole.[2] However, our generalization is also motivated from more formal considerations *viz* working with a more general class of gauges, which we discuss in appendix A.

---

[2]In this latter respect $\mathcal{V}_{qq}$ differs from the dipole splitting functions of [15]: reproducing the eikonal limit of the colour dipole requires a sum of *two* dipole splitting functions.

2.5 Sudakov form factor and shower algorithm

Proceeding with strong ordering and quasi-collinear factorization as simplifying assumptions, this corresponds to working in the leading-log approximation. It is well known that large logarithms associated to collinear and soft emissions must vanish when the full phase-space is integrated over, this is a consequence of the Block-Nordsieck and KLN theorems. We may use this fact to rewrite the integrals over the phase space for unresolved gluon emissions $\mathcal{U}$ (where we take $\mathcal{U}$ to be the region $z > z_c$ where z_c is some cut-off) in terms of integrals over the remaining resolved gluon phase-space $\mathcal{R}$, specifically we use,

$$\int_{\mathcal{U}} \mathrm{d}P_i\,(t \to tg) + \int_{\mathcal{R}} \mathrm{d}P_i\,(t \to tg) = 0 \tag{2.25}$$

where

$$\int_{\mathcal{U}/\mathcal{R}} \mathrm{d}P_i\,(t \to tg) = \int_{\tilde{q}_{i-1}^2}^{\tilde{q}_{\max}^2} \mathrm{d}\tilde{q}_i^2 \mathrm{d}z_i\, \frac{\alpha_{\mathrm{S}}}{2\pi\tilde{q}_i^2} P_{qq}\left(z_i, \tilde{q}_i^2\right) \Theta\left(\mathcal{U}/\mathcal{R}\right), \tag{2.26}$$

and $\Theta\left(\mathcal{U}/\mathcal{R}\right) = 1$ for gluon emissions in $\mathcal{U}/\mathcal{R}$ and zero otherwise. This gives the following expression for the decay width, with n *unresolved* branchings,

$$\int \mathrm{d}\Gamma_n = \prod_{i=1}^{n} \left(-\int_{\mathcal{R}} \mathrm{d}P_i\,(t \to tg) \right) \frac{1}{2m_t} \int \mathrm{d}\Phi_{bW}\,(2\pi)^4\,\delta^4\left(q_{t,n} - q_b - q_W\right) |\mathcal{M}_0|^2. \tag{2.27}$$

Within leading-log accuracy we may neglect the dependence of the final decay, to the b-quark and W boson, on $q_{t,n}$. Such approximations are a generic feature of all leading-log parton shower simulations. With this in mind we may simply rewrite the nested integrals over the branching probabilities as

$$\int \mathrm{d}\Gamma_n = \tfrac{1}{n!} \left(-\int_{\mathcal{R}} \mathrm{d}P_1\,(t \to tg) \right)^n \int \mathrm{d}\Gamma_0. \tag{2.28}$$

Summing over all n, the corrections due to unresolved gluon emission exponentiate to give, in the leading-log approximation,

$$\Gamma_{\mathcal{U}} = \exp\left(-\int_{\mathcal{R}} \mathrm{d}P_1\,(t \to tg) \right) \int \mathrm{d}\Gamma_0. \tag{2.29}$$

Since all soft and collinear logarithmic corrections to the width must vanish on integrating over the entire phase-space $\mathcal{R} + \mathcal{U}$, in the leading log approximation the total width is simply equal to that given by the leading-order calculation: Γ_0. Hence, the probability that the top quark *evolves* from scale $\tilde{q}_0^2$ to $\tilde{q}_{\max}^2$ without emitting any resolvable radiation is,

$$\Delta\left(\tilde{q}_0^2, \tilde{q}_{\max}^2\right) = \frac{\Gamma_{\mathcal{U}}}{\Gamma_0} = \exp\left(-\int_{\mathcal{R}} \mathrm{d}P_1\,(t \to tg) \right), \tag{2.30}$$

the Sudakov form factor. By the same token $\mathrm{d}P_i$ represents the probability of a branching $t \to tg$ with z_i in the interval $[z_i, z_i + \mathrm{d}z_i]$ and $\tilde{q}_i^2$ in $\left[\tilde{q}_i^2, \tilde{q}_i^2 + \mathrm{d}\tilde{q}_i^2\right]$, for resolvable gluons.[3] The same calculations hold for the b-quark.

---

[3]With this interpretation (2.25) implies that this same probability $\mathrm{d}P_i$ is negative in the unresolvable region. Clearly the interpretation of $\mathrm{d}P_i$ as a probability in this region is not sensible, however the minus sign is expected, it is known to originate from the virtual gluon emissions (loop contributions), which are of course unresolvable emissions.

With these results we find the probability that the top quark evolves from scale $\tilde{q}_i^2$ to $\tilde{q}_{\max}^2$ without emitting any radiation is

$$S\left(\tilde{q}_i^2, \tilde{q}_{\max}^2\right) = \frac{\Delta\left(\tilde{q}_0^2, \tilde{q}_{\max}^2\right)}{\Delta\left(\tilde{q}_0^2, \tilde{q}_i^2\right)}. \qquad (2.31)$$

Therefore the probability that there is some resolvable radiation emitted as the top quark evolves from scales $\tilde{q}_i^2$ to $\tilde{q}_{\max}^2$ is $1 - S\left(\tilde{q}_i^2, \tilde{q}_{\max}^2\right)$, which may be written as

$$-\int_{\tilde{q}_i^2}^{\tilde{q}_{\max}^2} \mathrm{d}\tilde{q}^2 \, \frac{\mathrm{d}S\left(\tilde{q}_i^2, \tilde{q}^2\right)}{\mathrm{d}\tilde{q}^2} = \int_{\tilde{q}_i^2}^{\tilde{q}_{\max}^2} \mathrm{d}\tilde{q}^2 \mathrm{d}z \, \frac{\alpha_{\mathrm{S}}}{2\pi\tilde{q}^2} P_{qq}\left(z, \tilde{q}^2\right) S\left(\tilde{q}_i^2, \tilde{q}^2\right) \Theta\left(\mathcal{R}\right). \qquad (2.32)$$

The integrand of (2.32) is the probability density that the next resolvable branching after $\tilde{q}_i^2$ occurs at scale $\tilde{q}^2$.

The probability distribution (2.32) is sampled using the veto algorithm as described in [6]. Finally we note that, the gluons produced by the top quark and bottom quark will in turn produce their own parton showers; these showers are standard time-like gluon showers, not subject to any complications, e.g. initial-state evolution or parton masses, as is the case for the top quark shower, the details of such gluon showering are described in [5].

2.6 Phase-space limits - boundary conditions

We will now discuss the integration limits for the Sudakov form factor starting with z. The boundaries on the z variable depend on the $\tilde{q}^2$. For a given $\tilde{q}^2$ the z boundaries are determined by the requirement that $\mathbf{p}_\perp^2 > 0$. In the case of the top quark the requirement that the intermediate top quark has a mass greater than $(m_b + m_W)^2$ provides a further constraint on z. The implementation of these complicated z bounds is straightforward using the veto algorithm [6].

The lower bound on $\tilde{q}^2$ for both top and bottom quarks is simply $\tilde{q}^2 = m_q^2$ due to the fact that the top quark is initially on-shell and the final b-quark must also be on-shell. The phase-space boundaries in the $\tilde{q}^2$ variable were calculated in [5]. It was shown in [5], that for a given $\tilde{q}_{b,max}$ there is an upper bound $\tilde{q}_{t,max}$, for emissions from the top quark,

$$\left(\tilde{q}_{t,max}^2 - m_t^2\right)\left(\tilde{q}_{b,max}^2 - m_b^2\right) = \tfrac{1}{4}\left(m_t^2 - m_W^2 + m_b^2 + \lambda\right)^2, \qquad (2.33)$$

that partitions the phase-space for the decay $t \to bW + g$ into three regions which do not overlap: one region accessible to gluon emissions from the bottom quark, one accessible to emissions from the top quark, and a further inaccessible *dead region*.

This partitioning is vital to ensure that each phase space point has a unique matrix element approximation assigned to it and to avoid double counting of phase-space points. As such the three regions do not overlap, this is particularly significant for the soft gluon region of phase space, which is most heavily populated. The price to be paid for this partitioning is the presence of the dead region, however this region is solely comprised of high $\mathbf{p}_\perp$ gluons, so it is sparsely populated, and in any case the parton-shower approximation is known to model such emissions badly.
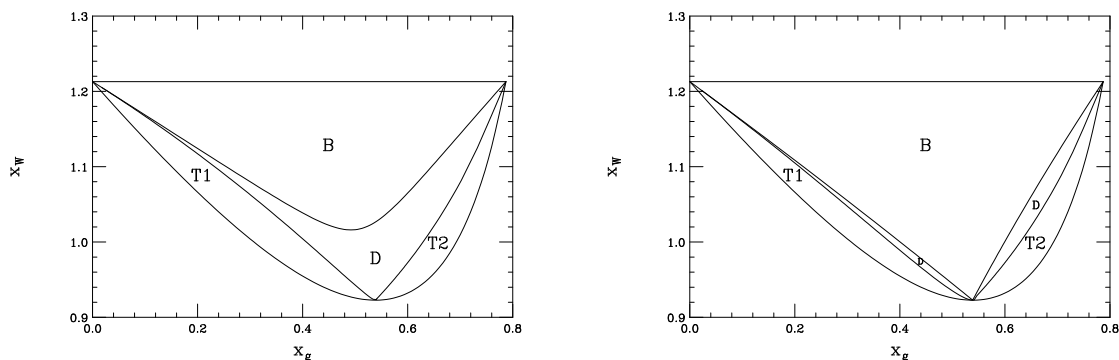
Figure 3: In this figure we show the phase space boundaries for the *symmetric* (left) and *maximal* (right) choices of phase space partitioning, in the x_g, x_W plane, where x_g and x_W are equal to two times the energy fraction of the gluon and W boson in the top quark rest frame. The regions T1 and T2 are populated by gluon emissions from the top quark while the region labelled B is populated by emissions from the b-quark. The region labelled D is the *dead region*. For the *symmetric* choice the phase space volume is divided more or less evenly between that accessible to emissions from the top and bottom quarks, while the *maximal* choice maximises the volume to be populated by emissions from the b-quark.

Given the relation (2.33), between $\tilde{q}^2_{t,max}$ and $\tilde{q}^2_{b,max}$, we define two choices of phase-space partition, the so-called *symmetric* choice,

$$\tilde{q}^2_{b,max} = m_b^2 + \tfrac{1}{2}\left(m_t^2 - m_W^2 + m_b^2 + \lambda\right) \tag{2.34}$$

and *maximal* choice

$$\tilde{q}^2_{b,max} = 4\left((m_t - m_W)^2 - m_b^2\right). \tag{2.35}$$

In the case of the *symmetric* choice, the phase-space volume is divided more or less evenly between that accessible to emissions from the top and bottom quarks, while the *maximal* choice maximises the volume to be populated by emissions from the b-quark. The two choices of phase-space partitioning can be seen in figure 3. Typically we favour the *symmetric* choice, as the *maximal* choice involves generating high transverse momentum emissions from the b-quark.

2.7 Kinematics reconstruction

Given the boundary conditions and the emission probability distribution (2.32) we have all we need to generate parton showers in terms of $\tilde{q}_i^2$, z_i and ϕ_i. The Sudakov variable α_i may be calculated from (2.4) as each z_i is generated, the transverse momentum is also calculated at this point. The calculation of the β_i variables is more complicated.

For time-like, final-state, showers we start at the end of the shower, since the particles are on-shell there we can simply determine the value of β_i by computing q_i^2 from (2.1) and setting $q_i^2 = m_q^2$, where m_q^2 is the on-shell mass squared. Once this is done the *parent* particle's virtuality, and hence its β_i value, follows directly from momentum conservation.

– 13 –

Applying momentum conservation to each vertex in such showers, one can fully reconstruct all of the momenta up to and including that of the *shower progenitor particle*.

Recall that the gluons radiated by the top quark will produce their own time-like showers. The first step in reconstructing the momenta of the top quark as it evolves toward its decay, is to reconstruct these showers, i.e. we first reconstruct the momenta of the gluons that were radiated by the top quark by applying the procedure outlined above. The momentum of the top quark after each gluon emission can then be calculated by momentum conservation, as the initial top quark momentum is known $(m_t, \mathbf{0}, 0)$. In this way we completely determine the momenta of the top quark and all of the radiation emitted prior to the $t \to bW$ decay. Should the b-quark also emit radiation, the resulting jet(s) will be reconstructed in the standard way for time-like showers [6].

Since the initial b and W boson momenta were generated according to the tree level $t \to bW$ decay they add up to $(m_t, \mathbf{0}, 0)$, rather than the actual momentum of the top quark prior to its decay. Furthermore, if the b-quark radiates, forming a b-jet[4] the jet reconstruction described above leads to the initial b-quark momentum having a virtuality greater than its mass.

In order to ensure global momentum conservation we perform a 'momentum reshuffling' which smoothly preserves the internal properties of each jet. Let us denote the total momentum of the jets radiated by the top quark g_{ISR}. The first step in the momentum reshuffling involves rescaling the three-momenta of the W boson to account for the loss of energy due to gluon emissions from the top quark. The second step involves absorbing the component of g_{ISR} transverse to the W, in the b-jet. Finally the momentum of the b-jet in the direction of the original b-quark is rescaled. This process is sketched in figure 4 and is described by the following mapping:

$$
\begin{aligned}
q_W &= \left(\sqrt{m_W^2 + \mathbf{p}^2}, -\mathbf{p}\right) \to \left(\sqrt{m_W^2 + k_2^2 \mathbf{p}^2}, -k_2 \mathbf{p}\right), \\
q_{b_{JET}} &= \left(\sqrt{m_{b_{JET}}^2 + \mathbf{p}_{b_{JET}}^2}, \mathbf{p}_{b_{JET}}\right) \to \left(\sqrt{m_{b_{JET}}^2 + k_1^2 \mathbf{p}^2 + \mathbf{p}_{ISR\perp}^2}, k_1 \mathbf{p} - \mathbf{p}_{ISR\perp}\right),
\end{aligned}
\tag{2.36}
$$

where $\mathbf{p}$ is the initial W boson momentum from the $t \to bW$ process, k_1 and k_2 are constant rescalings of the b-jet and W boson momenta. The three vectors $\mathbf{p}_{ISR\parallel}$ and $\mathbf{p}_{ISR\perp}$ are the components of g_{ISR} parallel and perpendicular to $\mathbf{p}$. Applying energy-momentum conservation to the momenta above allows one to determine the value of the rescalings k_1 and k_2. The top quark and the radiation from it are untouched by the momentum reshuffling.

In practice, rather than applying the rescalings and momentum subtractions as indicated in (2.36), once k_1 and k_2 are determined we actually calculate the Lorentz boosts which perform a mapping that is exactly equivalent to that in (2.36). By calculating the mapping in terms of these Lorentz boosts, we can conserve momentum and preserve the internal structure of the jets by applying the boosts to each particle in the b-quark jet.

If the top quark does not radiate any gluons before decaying, the three-momenta of the b-jet and W boson system are rescaled such that its invariant mass is equal to the top mass. In this special case the problem of momentum reshuffling is identical to that of

---

[4]In the present discussion we will assume the b-quark has given rise to a jet since this is the general case, the extension to the case where it does not radiate is trivial.
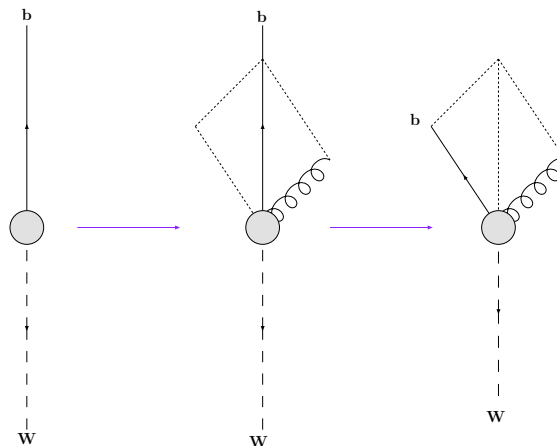
Figure 4: In this figure we sketch the 'momentum reshuffling' procedure. Initially the top quark decay to a b-quark and a W boson is simulated, this momentum configuration is shown first on the far left. Afterwards some additional radiation is produced from the parton shower, represented by the spiral in the central configuration above, clearly this configuration does not conserve momentum. The initial b-jet momenta are rescaled and boosted to give the configuration shown on the right hand side: the three-momenta of the W boson and b-jet are scaled down and the momentum of the additional radiation, transverse to the W-boson direction, is absorbed by the b-jet .

$e^+e^- \to q\bar{q}$ events, hence for these cases we use exactly the same momentum reshuffling as described in [6].

This sequence of boosts and rescalings is designed such that, at least for the case of one gluon emission, the 3-body decay kinematics of [5] are reproduced, i.e. should the gluon be emitted by the top quark, or the b-quark, its transverse momentum is absorbed by the b-quark, in the top quark rest frame (as depicted in figure 4).

3. Matrix element corrections

As stated in section 2, the effects of unresolvable gluon emissions have been included to all orders through the Sudakov form factor. The master formula and shower algorithms generate further resolvable emissions by approximating the full $t \to bW + (n)\,g$ matrix element by a product of quasi-collinear splitting functions multiplying the tree level amplitude. Ideally, we wish to include the higher-order effects in the master equation as accurately as possible.

3.1 Soft matrix element corrections

In the parton shower approximation the probability density that the ith resolvable gluon is emitted into $\left[\tilde{q}^2, \tilde{q}^2 + \mathrm{d}\tilde{q}^2\right], [z, z + \mathrm{d}z]$ is

$$dP\left(z, \tilde{q}^2\right) = \frac{\mathrm{d}\tilde{q}^2}{\tilde{q}^2}\mathrm{d}z\, \frac{\alpha_\mathrm{S}\left(\mathbf{p}_T\right)}{2\pi} P_{qq}\left(z, \tilde{q}^2\right)\Theta\left(\mathcal{R}\right). \tag{3.1}$$

This approximation works well for the case that the emission lies within the domain of the quasi-collinear limit. On the other hand the exact matrix element calculation gives us that the probability of a resolved emission is (at least in the leading log approximation)

$$\int_{\mathcal{R}} \mathrm{d}P^{\mathrm{m.e.}} = \int \mathrm{d}\tilde{q}^2 \mathrm{d}z \, \frac{1}{\Gamma_0} \frac{\mathrm{d}^2\Gamma}{\mathrm{d}z \mathrm{d}\tilde{q}^2} \Theta(\mathcal{R}), \tag{3.2}$$

where Γ is the width of the process $t \to bWg$. The differential width for $t \to bWg$ is given in appendix B.2. Once again the 'probability' of an unresolved emission can therefore be written $- \int_{\mathcal{R}} \mathrm{d}P^{\mathrm{m.e.}}$, proceeding in the same way as our earlier derivations (2.32), we then have the probability density that the ith resolvable gluon is emitted into $[\tilde{q}^2, \tilde{q}^2 + \mathrm{d}\tilde{q}^2]$, $[z, z + \mathrm{d}z]$ is given by the integrand of

$$\int_{\tilde{q}_{i-1}^2}^{\tilde{q}_{\mathrm{max}}^2} \mathrm{d}\tilde{q}_i^2 \mathrm{d}z \, \frac{1}{\Gamma_0} \frac{\mathrm{d}^2\Gamma}{\mathrm{d}z \mathrm{d}\tilde{q}_i^2} \, \exp\left(- \int_{\tilde{q}_{i-1}^2}^{\tilde{q}_i^2} \mathrm{d}\tilde{q}^2 \mathrm{d}z \, \frac{1}{\Gamma_0} \frac{\mathrm{d}^2\Gamma}{\mathrm{d}z \mathrm{d}\tilde{q}^2} \right). \tag{3.3}$$

We may generate the distribution in (3.3) by simply augmenting the veto algorithm that is used to produce (2.32) with a single additional rejection weight, simply vetoing emissions if a random number $\mathcal{R}_S$ is such that

$$\mathcal{R}_S \geq \left. \frac{\mathrm{d}P^{\mathrm{m.e.}}}{\mathrm{d}P} \right|_{z, \tilde{q}^2}. \tag{3.4}$$

For this to work we require that the parton shower emission probability $\mathrm{d}P$ always overestimates that of the exact matrix element $\mathrm{d}P^{\mathrm{m.e.}}$, if necessary this can be achieved by simply enhancing the emission probability of the parton shower with a constant factor.

In practice we do not apply this correction to all emissions as most should be well approximated by the parton shower. The emissions which are not expected to be modelled well are neither soft nor collinear, they have large transverse momentum ($\mathbf{p}_\perp$). In practice we make the ansatz that all emissions which do not have the largest $\mathbf{p}_\perp$ of any generated thus far, are considered to be infinitely soft and we only correct the set which is comprised of those emissions which have the largest $\mathbf{p}_\perp$ *so far*, to the full matrix element distribution.

One might be concerned that in this case it is really only proper to apply this correction to the final, largest $\mathbf{p}_\perp$ emission, however, in the context of our coherent parton branching formalism (angular ordering) the earlier wide angle emission is considered too soft to resolve the subsequent, larger $\mathbf{p}_\perp$ splitting, and is therefore effectively distributed assuming that the latter emission did not occur. Under these assumptions the correct procedure should be to correct only those emissions which are the hardest so far, from distribution (3.1) to distribution (3.3) by applying veto in (3.4) [8].

3.2 Hard matrix element corrections

In addition to correcting the distribution of radiation inside the T1, T2 and B regions populated by the parton shower, we also wish to correct the distribution of radiation outside, in the high $\mathbf{p}_\perp$ dead region. We wish to distribute the radiation in the dead region according to the full $t \to bWg$ matrix element i.e. according to

$$\frac{1}{\Gamma_0} \frac{\mathrm{d}^2\Gamma}{\mathrm{d}x_g \mathrm{d}x_W} = \frac{\alpha_S C_F}{\pi} \left(\frac{f(b, w, \tilde{q}^2, z)}{\lambda (1 + w - b - x_W) x_g^2} \right), \tag{3.5}$$

where $b = m_b^2/m_t^2$, $w = m_W^2/m_t^2$ and λ is given by (2.3). The full expression for the width is lengthy and so we give it in appendix B.2.

The first step in the algorithm is to generate a point inside the dead region. This is non-trivial as the phase-space boundaries shown in figure 3 are rather complicated functions of the mass of the b-quark, W-boson, z and $\tilde{q}^2$. It turns out that the phase-space may be parametrized as functions $x_W\left(x_g, \tilde{q}^2\right)$, that is, the Dalitz variable $x_W = 2q_W.p_t/m_t^2$ may be written as a function of $x_g = 2q_g.p_t/m_t^2$ and the evolution variable $\tilde{q}^2$(to do this one eliminates z in favour of x_g). These functions were calculated using the conventions in [5] and are noted in appendix B.1.

The phase-space point is selected by importance sampling the differential distribution (2.10) assuming a $x_g^{-\alpha}\left(1 + w - x_W\right)^{-1}$ behaviour, where α is a parameter which may be tuned to improve the sampling efficiency. First we rewrite the integral over the dead region (D) as,

$$
\begin{aligned}
\frac{1}{\Gamma_0} \int_D \mathrm{d}x_g \mathrm{d}x_W \, \frac{\mathrm{d}^2\Gamma}{\mathrm{d}x_g \mathrm{d}x_W} &= \frac{1}{\Gamma_0} \int_D \mathrm{d}y_g \mathrm{d}y_W \, \mathcal{W}\left(x_g, x_W\right), \\
\mathcal{W}\left(x_g, x_W\right) &= x_g^\alpha \left(1 + w - x_W\right) \frac{\mathrm{d}^2\Gamma}{\mathrm{d}x_g \mathrm{d}x_W}, \\
y_g &= \frac{1}{1-\alpha} x_g^{1-\alpha}, \\
y_W &= \ln\left(1 + w - x_W\right),
\end{aligned}
\tag{3.6}
$$

and generate y_g, y_W points assuming they are uniformly distributed between their maximum and minimum values in the dead region. Then we keep events with probability

$$
\mathcal{P} = \frac{\mathcal{W}(x_g, x_W)\mathcal{V}(y_g)}{\Gamma_0},
\tag{3.7}
$$

$(\mathcal{P} \le 1)$ where

$$
\mathcal{V}\left(y_g\right) = \left(y_{g,max} - y_{g,min}\right)\left(y_{W,max} - y_{W,min}\right)\big|_{y_g},
\tag{3.8}
$$

is the Monte Carlo estimate of the volume of the dead region in y_g, y_W plane: $y_{g,max}$ and $y_{g,min}$ are the maximum and minimum possible values for y_g in the dead region, while $y_{W,max}$ and $y_{W,min}$ are the maximum and minimum possible values of y_W in the dead region, for the generated value of y_g.

Once a pair of values y_g, y_W has been successfully generated, they may be mapped back to the corresponding x_g, x_W phase-space point and the momenta of the top quark, bottom quark and W boson can be constructed from there.

4. Results

In figure 5 we show the Dalitz distributions for the process $t \to bWg$ as given by the parton shower algorithm, including matrix element corrections. Only decays where *one* gluon is emitted are considered, since to do otherwise would constitute a different (higher dimensional) phase-space volume to that shown.

The Dalitz plots show significant clustering of events in the soft $x_g \to 0$ region as expected. One can also see a marked clustering of events along the line $x_W \approx 1.2$ where the energy fraction of the W boson is *maximal* i.e. where the gluon is emitted collinear with the b-quark. Again, this is to be expected since we know that collinear emissions
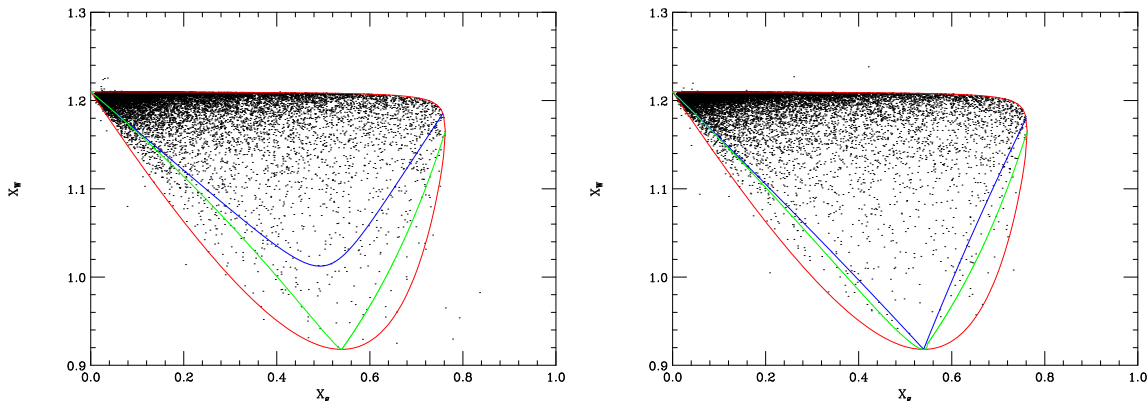
Figure 5: Dalitz plot for gluonic radiation in top decay. In both plots the soft and hard matrix element corrections have been applied, but only one emission has been allowed. a) shows the radiation for the symmetric choice of [5] for emission from the top and bottom while b) shows the radiation with the scales chosen to give the maximum amount of radiation from the bottom quark. The blue (innermost) line gives the limit for radiation from the bottom, the green (middle) line from the top and the red (outer) line the boundary of the phase space region.

from the b-quark are enhanced by logarithms of m_b^2/m_t^2. We do not see a similar wedge-like clustering of events at low transverse momentum with respect to the top quark. Such events would lie along the lower section of the red boundary between $x_g \approx 0$ and $x_g \approx 0.75$. Clustering along this line would only come from collinear enhancements of the form $\log \frac{Q^2}{m_t^2}$ where Q^2 is some hard scale, but in this case $Q^2 = m_t^2$ so there is no such enhancement, only soft enhancements $\log \frac{m_t^2}{m_g^2}$ giving rise to the observed clustering as $x_g \to 0$.

In addition to considering the isolated decay process we have also considered the process $e^+e^- \to t\bar{t}$ near threshold: $\sqrt{s} = 360\,\text{GeV}$. By working close to the $t\bar{t}$ threshold we inhibit the effects of radiation from the production phase of the $t\bar{t}$ pair, thus highlighting the effects of radiation in the $t\bar{t}$ decays. In analysing these events we have worked at the parton level and only considered leptonic W decays. We have clustered all final-state quarks and gluons into three jets using the $k_\perp$ clustering algorithm [16], taking care to omit the W decay products from the clustering. Events for which the minimum jet separation is less than $\Delta R = 0.7$ $\left(\Delta R^2 = \Delta\eta^2 + \Delta\phi^2\right)$, as well as events containing a jet with transverse energy less than $10\,\text{GeV}$, are excluded from the analysis. For these events we have plotted the distributions of the jet separation ΔR and the logarithm of the jet measure y_3, where

$$y_3 = \frac{2}{s}\,\min_{ij}\left(\min\left(E_i^2, E_j^2\right)(1 - \cos\theta_{ij})\right) \tag{4.1}$$

is the value of the jet resolution parameter for which the three jet event would be seen as a two jet event. This analysis is the same as that performed in two earlier related works [3, 17].

In figure 6 we show differential distributions with respect to the jet separation of the closest pair of jets in the event (ΔR), for the cases of the *symmetric* and *maximal* phase space partitions (2.34), (2.35). Figure 6 shows that the matrix element corrections have
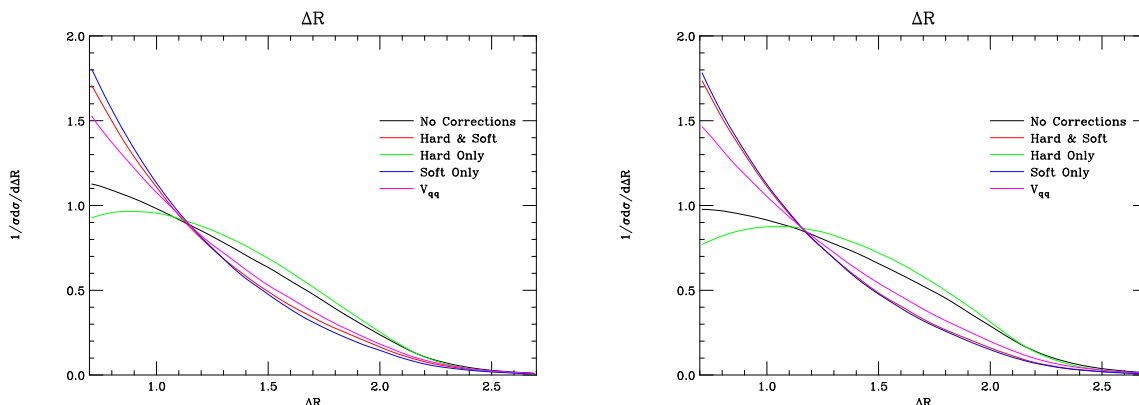
Figure 6: $\frac{1}{\sigma}\frac{d\sigma}{d\Delta R}$ where $\Delta R^2 = \Delta\eta^2 + \Delta\phi^2$ for three jet $e^+e^- \to t\bar{t}$ events at $\sqrt{s} = 360\,\mathrm{GeV}$ with and without matrix element corrections. On the left we show the distributions obtained for the case that the phase-space volume populated by the parton showers from the top and bottom quarks is almost the same size (the *symmetric* phase space partition (2.34)), while on the right we show the distributions obtained for the case that the shower from the b-quark populates most of the phase space choice (the *maximal* phase space partition (2.35)). In each plot the black line corresponds to the parton shower approximation, the red line corresponds to the parton shower including hard and soft matrix element corrections, while the green/blue lines respectively correspond to including only the hard/soft part of the matrix element corrections. The magenta line is obtained using the standalone parton shower but with P_{qq} replaced by the generalized quasi-collinear splitting function $\mathcal{V}_{qq}$ (2.24).

significant consequences for the ΔR distributions. We see that when the soft matrix element correction is applied, the distribution is more peaked for small ΔR and tails off more quickly than the distributions obtained without it. This is to be expected, it is a *softening* of the distribution, it is indicative of the fact that the soft matrix element correction is vetoing a number of high p_T emissions, not well modelled by the standalone parton shower: such hard emissions naturally give rise to more widely separated jets (larger ΔR).

The degree to which the soft matrix element correction affects the ΔR distribution suggests that the standalone parton shower does not model the number of these high p_T emissions well: similar distributions were observed in version 5.9 of the older HERWIG program and were since considered to be the result of a bug (showering in the wrong reference frame). In our case the effect shown is understood to be a genuine artefact of the covariant parton shower formalism and may be traced back to the form of the quasi-collinear splitting function for b-quark emissions. In section 2.4 we noted that, as the angle between the reference vector (n) and the emitted gluon (k) decreases, emissions will be enhanced in the n direction (particularly soft emissions). This spurious enhancement results from choosing n not equal to precisely the momentum of the colour partner of the b-quark. This also explains why the differences between the results with and without matrix element corrections are more pronounced for the *maximal* phase space partition than the *symmetric* partition. On the contrary our results including the soft matrix element corrections compare well with those obtained in the earlier FORTRAN HERWIG program.
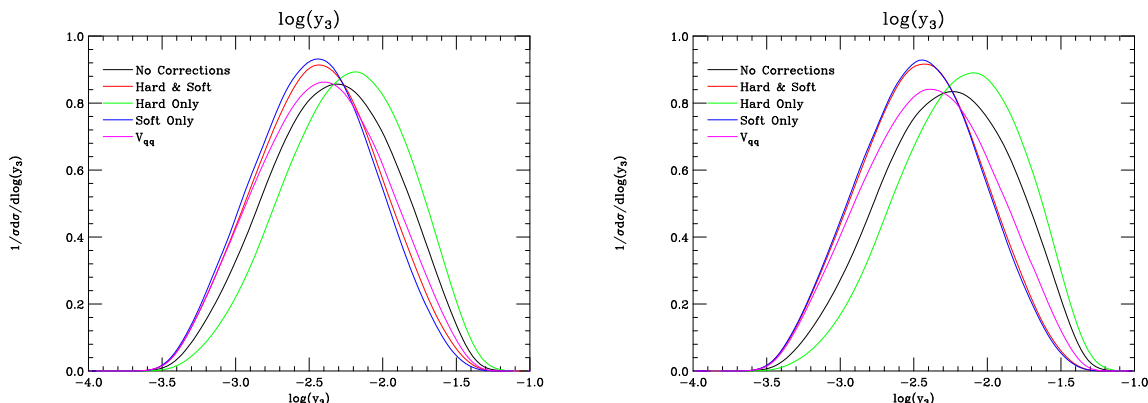
Figure 7: $\frac{1}{\sigma}\frac{\mathrm{d}\sigma}{\mathrm{d}\log(y_3)}$ where $y_3 = \frac{2}{s}\,\min_{ij}\left(\min\left(E_i^2, E_j^2\right)\left(1 - \cos\theta_{ij}\right)\right)$ for three jet $e^+e^- \to t\bar{t}$ events at $\sqrt{s} = 360\,\mathrm{GeV}$ with and without matrix element corrections. As in figure 6, on the left we show the distributions obtained for the *symmetric* phase space partition (2.34), while on the right we show the distributions obtained for the *maximal* phase space partition (2.35). The histograms are coloured in the same way as for figure 6.

In section 2.4 we also proposed a new generalized quasi-collinear splitting function $\mathcal{V}_{qq}$ (see also appendix A), which improves on the usual quasi-collinear splitting function by reducing to the eikonal dipole function in the soft limit. From a practical point of view the introduction of this splitting function is akin to a soft matrix element correction. The ΔR distributions support this assertion; the standalone parton shower is greatly improved by the use of this new splitting function.

As with figure 6, in figure 7 we show differential distributions with respect to the jet measure y_3, for the cases of the *symmetric* and *maximal* phase space partitions, for all possible combinations of matrix element corrections. We also show the same distribution obtained using the generalized quasi-collinear splitting function in the basic parton shower. When the soft matrix element correction is applied, the distribution shifts toward smaller y_3 values since some high p_T emissions will be vetoed by it. Conversely the hard matrix element correction supplies more events with high p_T emissions and so the distribution shifts toward higher y_3 values, since these events will not require such fine resolution to distinguish three jets from two jets. As with the ΔR distributions, the introduction of the generalized quasi-collinear splitting functions, $\mathcal{V}_{qq}$, gives a substantial improvement of the basic parton shower, softening the jet structure.

In figures 8 and 9 we see the effects of varying the choice of phase space partitioning, as well as the gluon mass parameter, on the ΔR and y_3 distributions. The distributions are less sensitive to changes in this parameter when the matrix element corrections are applied, compared to the case of the standalone parton shower. This is to be expected given that the quasi-collinear splitting functions (P_{qq}) are known to produce an excess of emissions as one approaches the acolinear direction. This explains the variation of the distributions on shifting the phase space boundary, moreover the majority of these spurious emissions will be soft, resulting in a heightened sensitivity to the gluon mass parameter.
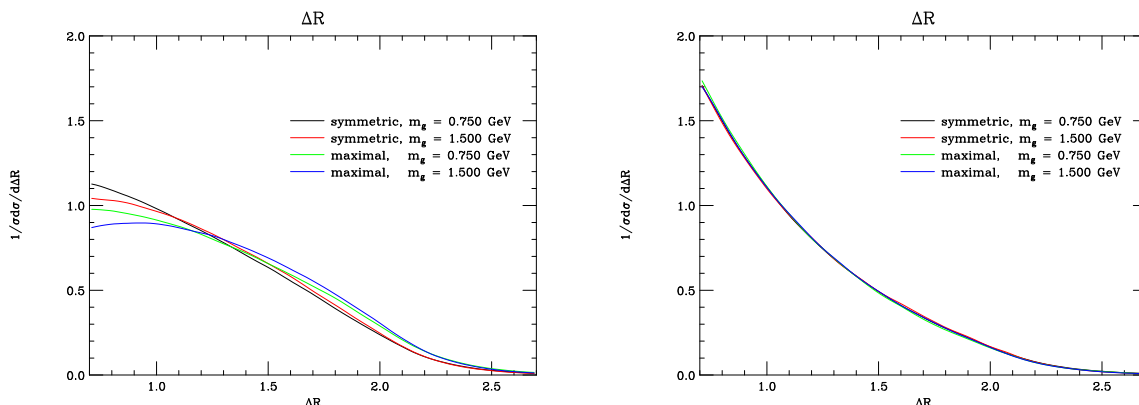
Figure 8: Here we show the $\frac{1}{\sigma}\frac{\mathrm{d}\sigma}{\mathrm{d}\Delta R}$ distribution as in figure 6. On the left we show the distribution obtained from the parton shower approximation and on the right we show the same distribution including all matrix element corrections. In each case we have shown how doubling the gluon mass and/or varying the choice of phase space partition affects the result.
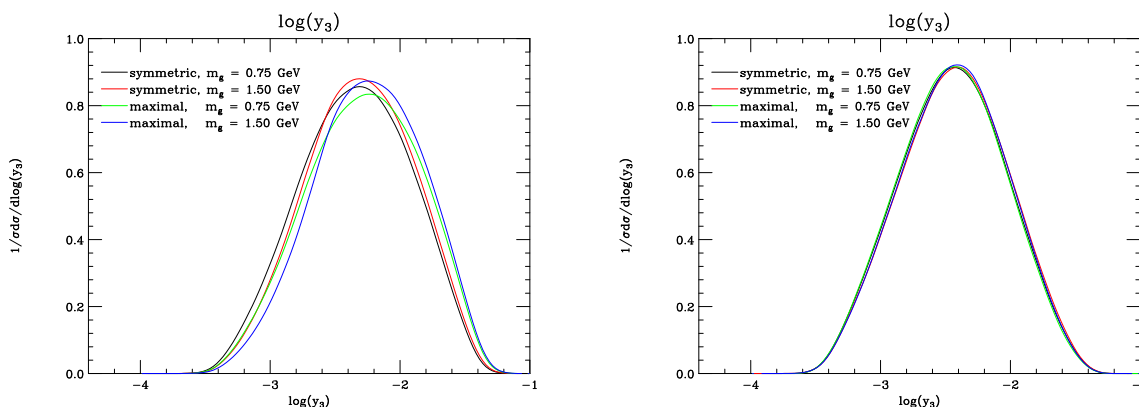

Figure 9: Here we show the $\frac{1}{\sigma}\frac{\mathrm{d}\sigma}{\mathrm{d}\log(y_3)}$ distribution as in figure 7. On the left we show the distribution obtained from the parton shower approximation and on the right we show the same distribution including all matrix element corrections. In each case we have shown how doubling the gluon mass and/or varying the choice of phase space partition affects the result.

5. Conclusions

At the beginning of this paper we presented a theoretical framework for the simulation of QCD radiation emitted in top quark decays. In section 2 we described the basic parton shower formulation. Although this formalism is the product of almost thirty years of evolution, it has not previously been applied to the extremes of kinematics and mass scales found in top decay. In doing so we find that the latest covariant parton shower formalism of [5] works well under these conditions and we have gained new insight regarding its use. In particular, we introduced a generalization of the quasi-collinear limit [13, 15] for which the $q \to qg$ splitting function correctly reproduces the eikonal limit.

In section 3 we have described the soft matrix element correction which fixes the

distribution of the *hardest* emission to be that of the leading-order matrix element for the decay $t \to bWg$, in a manner respecting colour coherence. We also describe the hard matrix-element correction which simply populates the dead region of phase space (not populated by the parton shower) according to the same single gluon emission matrix element.

The results of our program show good agreement with those of the FORTRAN HERWIG program for the ΔR and y_3 observables, provided that either the soft matrix element correction is applied [3], or our proposed generalization of the $q \to qg$ quasi-collinear splitting function is used (2.24). The associated Dalitz plots obtained for isolated $t \to bWg$ decays also meet with our expectations. Distributions obtained using the standalone parton shower with the conventional quasi-collinear splitting functions, suffer from an excess of high p_T emissions from the b-quark. This excess in the original basic shower formulation is well understood to arise from the choice of reference vector (n) required for the b-quark shower. Future versions of the Herwig++ program will use the new splitting function by default.

The simulation we have presented improves on that of the older HERWIG program in a number of ways through the use of the new covariant parton shower formalism. The new formalism brings with it the use of the quasi-collinear Altarelli-Parisi splitting functions, which lead to a natural screening of collinear singularities, allowing us to dispense with the *ad hoc* angular cut-off, which was responsible for the spurious *dead-cone halo*. Moreover, in this paper we propose a generalization of these splitting functions, leading to further improvements in the modelling of soft radiation. We have also been able to generate radiation from the top quark in its rest frame, thereby populating infrared regions, corresponding to soft gluon emissions from the top quark, with the parton shower. Previously such regions were populated according to a single emission matrix element correction with an arbitrary soft cut-off [3].

It is clear from our discussion that this work may be readily extended to decays of other heavy particles, in particular squarks and gluinos. Should supersymmetry be realised in nature, squark and gluino decays will give rise to a significant amount of activity in the LHC experiments, which we will need to simulate. Moreover, as with the top quark today, measuring the masses of these particles will be a major area of study, requiring accurate simulations of their decays. It is our intention to make this extension in a future version of the Herwig++ program.

Acknowledgements

A. Generalizing the $q \to qg$ quasi-collinear splitting function

The quasi-collinear limit is that in which $q_\perp$ becomes $\mathcal{O}(m_q)$ and small [15]. This region can be identified by the *uniform* rescalings $q_\perp \to \lambda q_\perp$, $m_q \to \lambda m_q$ and examining the limit $\lambda \to 0$. In the case of a quasi-collinear gluon emission from a quark, in an arbitrary n

particle process, the squared matrix element factorizes as

$$\lim_{q_i \| k_i} |\mathcal{M}_n|^2 = \frac{8\pi\alpha_{\mathrm{S}}}{q_{i-1}^2 - m_q^2} P_{qq} |\mathcal{M}_{n-1}|^2, \tag{A.1}$$

$$P_{qq} = C_F \left(\frac{1+z^2}{1-z} - \frac{m_q^2}{q_i.k_i} \right), \tag{A.2}$$

where $z = n.q_i/n.q_{i-1}$.

Note that, as well defining the Sudakov decomposition, the reference vector n also specifies a choice of axial gauge. Restricting the form of n imposes restrictions on the choice of axial gauge. To make calculations easier, n is typically chosen to be lightlike and perpendicular to $k_\perp$, as in [13]. The resulting splitting kernel (A.2) is invariant under gauge transformations respecting these constraints $\left(n^2 = n.k_\perp = 0\right)$ i.e. Lorentz boosts of n, in the n direction. Invariance under more general Lorentz transformations requires $k_\perp = 0$; in this sense $k_\perp$ may be regarded as a measure of the gauge dependence of approximation (A.1).

Parton shower simulations use approximation (A.1) beyond the collinear limit, so strictly speaking the approach is not gauge invariant. This is not a problem provided that gauge dependent contributions are sub-leading. However, in the case of the b-quark shower we have noted an excess of emissions at the edge of the shower phase space, due to an unphysical singularity, proportional to $n.k_i^{-1}$, where n is collinear with the W boson. Furthermore, as discussed in section 2.4, in the limit of soft emissions the splitting kernel (A.1) does not reduce to the correct eikonal dipole radiation function.

What we require is that the splitting kernel reproduces the correct collinear and (ideally) soft limits of the matrix element, without introducing any other singular terms. Since the behaviour of matrix elements in these limits is universal, any splitting kernel satisfying these criteria will be, at least to leading order, gauge invariant.

It turns out that all of these problems can be solved by simply relaxing the restrictions on the gauge vector. It is well known that the eikonal limit of a colour dipole can be calculated by considering gluon emission from just one quark, provided that the gauge vector is equal to the momentum of the colour partner. In order to reproduce the correct soft behaviour we should therefore always set the gauge vector equal to the four-momentum of the colour partner of the emitter. Although one can often obtain a good approximation to the eikonal limit by choosing n to be lightlike and collinear to the colour partner, if the colour partner is heavy, as in top decay, this approximation fails.

In any case, this prompts us to consider the case that n is massive. If we do this we find that the steps leading to (A.1) now give, up to sub-leading terms,

$$P_{qq} \to \mathcal{V}_{qq} = C_F \left(\frac{1+z^2}{1-z} - \frac{m_q^2}{q_i.k_i} - \frac{n^2}{n.k_i} \left(\frac{q_i.k_i}{n.k_i} \right) \right), \tag{A.3}$$

with z *defined* as $z = n.q_i/n.q_{i-1}$. The additional term in the generalized quasi-collinear splitting function ($\mathcal{V}_{qq}$) directly arises from the n^2 term in the gluon polarization sum. The new splitting function $\mathcal{V}_{qq}$ (A.3) reproduces the correct soft and collinear limits in the shower phase space, it contains no unphysical divergent terms.

From a purely pragmatic point of view $\mathcal{V}_{qq}$ can be considered as a kind of global soft matrix element correction and it is seen to have similar effects on physical observables (see section 4). Crucially, unlike the soft matrix element corrections, the generalized quasi-collinear splitting function is process-independent.

B. $t{\rightarrow}bWg$ phase-space and matrix element

In this appendix we give the matrix element for $t \rightarrow bWg$ decay and the phase-space parametrization, these are necessary for the hard matrix element correction discussed in section 3. Both the phase-space and matrix element are parametrized in terms of the Dalitz variables

$$x_i = \frac{2q_i.p_t}{m_t^2},\tag{B.1}$$

which, in the top quark rest frame, are equal to two times the fraction of the top quark's energy carried by particle i. We also define the following ratios of masses for convenience:

$$b = \frac{m_b^2}{m_t^2} \, , \, w = \frac{m_W^2}{m_t^2}.\tag{B.2}$$

B.1 Phase space

The Dalitz variables x_i, were calculated in [5], in terms of z and the top quark evolution variable $\tilde{\kappa}_t = \tilde{q}^2/m_t^2$, assuming the gluon was emitted by the top quark, as being

$$\begin{aligned}
x_W\left(z,\tilde{\kappa}_t\right) &= \tfrac{1+w-b-(1-z)\tilde{\kappa}_t-\sqrt{(1+w-b-(1-z)\tilde{\kappa}_t)^2-4w(1-(1-z)(\tilde{\kappa}_t-1))z}}{2z} \\
&\quad + \tfrac{1+w-b-(1-z)\tilde{\kappa}_t+\sqrt{(1+w-b-(1-z)\tilde{\kappa}_t)^2-4w(1-(1-z)(\tilde{\kappa}_t-1))z}}{2(1-(1-z)(\tilde{\kappa}_t-1))} \, , \\
x_g\left(z,\tilde{\kappa}_t\right) &= (1-z)\,\tilde{\kappa}_t,
\end{aligned}\tag{B.3}$$

where $b = m_b^2/m_t^2$ and $w = m_W^2/m_t^2$. We may completely eliminate z from x_W to give

$$\begin{aligned}
x_W\left(x_g,\tilde{\kappa}_t\right) &= \tfrac{1}{2(\tilde{\kappa}_t-x_g)}\left(\tilde{\kappa}_t\left(1+w-b-x_g\right)-\Lambda\left(x_g,\tilde{\kappa}_t\right)\right) \\
&\quad + \tfrac{1}{2(\tilde{\kappa}_t+x_g(1-\tilde{\kappa}_t))}\left(\tilde{\kappa}_t\left(1+w-b-x_g\right)+\Lambda\left(x_g,\tilde{\kappa}_t\right)\right), \\
\Lambda\left(x_g,\tilde{\kappa}_t\right) &= \sqrt{\left(x_g-\hat{x}_{g+}\right)\left(x_g-\hat{x}_{g-}\right)\left(\tilde{\kappa}_t-\tilde{\kappa}_+\right)\left(\tilde{\kappa}_t-\tilde{\kappa}_-\right)}, \\
\hat{x}_{g\pm} &= 1-\left(\sqrt{w}\pm\sqrt{b}\right)^2, \\
\tilde{\kappa}_\pm &= 2x_g\left(x_g\pm\sqrt{\left(1-\tfrac{1}{w}\right)\left(x_g-\bar{x}_{g+}\right)\left(x_g-\bar{x}_{g-}\right)}\right)^{-1}, \\
\bar{x}_{g\pm} &= \tfrac{(1-w)\left(1\pm\sqrt{w}\right)-b\left(1\mp\sqrt{w}\right)}{1-w}.
\end{aligned}\tag{B.4}$$

The expression for x_W given in (B.4) enables one to draw lines of constant $\tilde{\kappa}_t$ in the x_W, x_g plane.

Repeating the procedure for the case that the gluon is assumed to originate from the b-quark gives

$$\begin{aligned}
x_{g\pm}\left(x_W,\tilde{\kappa}_b\right) &= 2-x_W-z_\pm\left(x_W,\tilde{\kappa}_b\right)\sqrt{x_W^2-4w} \\
&\quad -\tfrac{1}{2}\left(1+\tfrac{b}{1+w-x_W}\right)\left(2-x_W-\sqrt{x_W^2-4w}\right), \\
z_\pm\left(x_W,\tilde{\kappa}_b\right) &= \tfrac{1}{2\tilde{\kappa}_b}\left(\tilde{\kappa}_b\pm\sqrt{\tilde{\kappa}_b^2-4\tilde{\kappa}_b\left(1+w-b-x_W\right)}\right).
\end{aligned}\tag{B.5}$$

Inverting (B.5) to obtain x_W as a function of x_g involves a high-order polynomial requiring a numerical solution, neglecting the b-quark mass an analytic solution becomes possible.

B.2 Matrix element

The matrix element for the decay $t \to bWg$ was given in [3, 5] assuming a massless b-quark. We calculate the squared matrix element, without neglecting the b-quark mass and find

$$
\begin{aligned}
\frac{1}{\Gamma_0}\frac{\mathrm{d}^2\Gamma}{\mathrm{d}x_g\mathrm{d}x_W} &= \frac{\alpha_S C_F}{\pi}\frac{1}{\lambda\bar{x}_W x_g^2} \\
&\left(-\frac{bx_g^2}{\bar{x}_W} + (1 - w + b)\, x_g - \bar{x}_W\, (1 - x_g) - x_g^2 \right. \\
&\left. + \frac{x_g}{1+w-2w^2-b(2-w-b)}\left(\tfrac{1}{2}\left(1 + 2w + b\right)\left(\bar{x}_W - x_g\right)^2 + 2w\bar{x}_W x_g\right)\right), \\
\bar{x}_W &= 1 + w - b - x_W
\end{aligned}
\tag{B.6}
$$

where again, $b = m_b^2/m_t^2$ and $w = m_W^2/m_t^2$. Setting $b = 0$, our expression (B.6) easily reduces to those given in [3, 5].

References

[1] S. Gieseke et al., *Herwig++ 2.0 release note*, hep-ph/0609306.

[2] S. Gieseke et al., *Herwig++ 2.0 beta release note*, hep-ph/0602069.

[3] G. Corcella and M.H. Seymour, *Matrix element corrections to parton shower simulations of heavy quark decay*, *Phys. Lett.* **B 442** (1998) 417 [hep-ph/9809451].

[4] G. Corcella et al., *Herwig 6.5 release note*, hep-ph/0210213.

[5] S. Gieseke, P. Stephens and B. Webber, *New formalism for QCD parton showers*, *JHEP* **12** (2003) 045 [hep-ph/0310083].

[6] S. Gieseke, A. Ribon, M.H. Seymour, P. Stephens and B. Webber, *Herwig++ 1.0: an event generator for e^+e^- annihilation*, *JHEP* **02** (2004) 005 [hep-ph/0311208].

[7] G. Marchesini and B.R. Webber, *Simulation of QCD coherence in heavy quark production and decay*, *Nucl. Phys.* **B 330** (1990) 261.

[8] M.H. Seymour, *Matrix element corrections to parton shower algorithms*, *Comp. Phys. Commun.* **90** (1995) 95 [hep-ph/9410414].

[9] I.I.Y. Bigi, Y.L. Dokshitzer, V.A. Khoze, J.H. Kuhn and P.M. Zerwas, *Production and decay properties of ultraheavy quarks*, *Phys. Lett.* **B 181** (1986) 157.

[10] V.A. Khoze, W.J. Stirling and L.H. Orr, *Soft gluon radiation in $e^+e^- \to t\bar{t}$*, *Nucl. Phys.* **B 378** (1992) 413.

[11] A. Bassetto, M. Ciafaloni and G. Marchesini, *Jet structure and infrared sensitive quantities in perturbative QCD*, *Phys. Rept.* **100** (1983) 201.

[12] R.K. Ellis, W.J. Stirling, and B.R. Webber, *QCD and collider physics*, *Camb. Monogr. Part. Phys. Nucl. Phys. Cosmol.* **8** (1996) 1.

[13] S. Catani, S. Dittmaier and Z. Trócsányi, *One-loop singular behaviour of QCD and SUSY QCD amplitudes with massive partons*, *Phys. Lett.* **B 500** (2001) 149 [hep-ph/0011222].

[14] D. Amati, A. Bassetto, M. Ciafaloni, G. Marchesini and G. Veneziano, *A treatment of hard processes sensitive to the infrared structure of QCD*, *Nucl. Phys.* **B 173** (1980) 429.

[15] S. Catani, S. Dittmaier, M.H. Seymour and Z. Trócsányi, *The dipole formalism for next-to-leading order QCD calculations with massive partons*, *Nucl. Phys.* **B 627** (2002) 189 [hep-ph/0201036].

[16] J.M. Butterworth, J.P. Couchman, B.E. Cox and B.M. Waugh, *KTJET: a C++ implementation of the K_t clustering algorithm*, *Comput. Phys. Commun.* **153** (2003) 85 [hep-ph/0210022].

[17] L.H. Orr, T. Stelzer and W.J. Stirling, *Gluon radiation in $t\bar{t}$ production and decay at the LHC*, *Phys. Rev.* **D 56** (1997) 446 [hep-ph/9609246].